Paleoenvironmental and paleoclimatic variations around Lake Van (Eastern Turkey) recorded by sedimentary source specific biomarkers 250- 130 ka (MIS7 and MIS6)

T. Guillemot[1, a], M. Stockhecke[1], A. Bechtel[2], S.N. Ladd[1, b], D.B. Nelson[1, c], C. J. Schubert[1*]

[1] Eawag, Swiss Federal Institute of Aquatic Science and Technology, Surface Waters – Research and Management, Kastanienbaum, Switzerland.

[2] Montanuniversitaet, Petroleum Geology, Leoben, Austria.

[a] present address: Paul Scherrer Institute, Villigen, Switzerland

[b] present address: Ecosystem Physiology, University of Freiburg, Freiburg, Germany

[c] present address: Department of Environmental Sciences – Botany, University of Basel, Basel, Switzerland

*corresponding author

Abstract

Paleoclimatic changes during MIS7 and MIS6 remain poorly described in the Near East. We quantified source-specific biomarkers in Lake Van sediments during the interglacial/glacial cycle MIS7/MIS6. Long-chain *n*-alkanes produced by land-derived vegetation, as well as long-chain alkenones and sterols (namely brassicasterol and dinosterol) produced by aquatic algae were investigated. Stable hydrogen isotopic measurements (δ^2H) on *n*-C_{29} alkanes were used as a proxy for aridity and revealed three wetter periods interrupted by two drier intervals during MIS7. In contrast, during the MIS6 glaciation, a generally drier climate was predominant. During the warmer and wetter periods of MIS7, a higher input of aquatic organic matter to Lake Van sediments was recorded by higher concentrations of long-chain alkenones, dinosterol and brassicasterol. Long-chain alkane abundances do not show a pattern related to aridity and were observed in higher concentrations in wetter as well as drier periods. Generally, in the Eastern Mediterranean, a wetter interglacial interrupted by drier episodes followed by a dry glacial period was the common feature observed during the MIS7/MIS6 interglacial/glacial cycle. However, in comparison to the last interglacial/glacial cycle the extreme dry glacial period registered around Lake Van from MIS5d to MIS2 was apparently unique and not equaled by a similar event within the last 250 ka.

Keywords: Lake Van, Quaternary, Middle East, Paleohydrology, Biomarkers, Compound specific hydrogen isotopes, Paleoclimatology, Organic geochemistry

1. Introduction

The Near East is a region where paleoenvironmental data are limited. Most available data focus on short geological timescales or are temporally discontinuous around the Mediterranean Sea (Gasse et al., 2011; Litt et al., 2014a; Rossignol-Strick and Paterne, 1999; Torfstein et al., 2009; Vaks et al., 2007; Miebach et al., 2019). Few studies from inland continental archives document climatic changes continuously over several interglacial/glacial cycles (e.g. Djamali et al., 2008). To enhance the knowledge of paleoclimatic variations in this region, the International Continental Drilling Project (ICPD) drilled several long sediment cores in Lake Van in 2010 (Litt et al., 2014b).

Located on the high plateau of eastern Anatolia near the border with Iran, Lake Van is the largest water body in Turkey and the largest (by volume) soda lake in the world (Litt et al., 2014b). Lake Van is a perfect site to reconstruct recent and past hydroclimatic variations for several reasons. First, sea level pressure anomalies promote northerly (and/or southerly) winds over Turkey (Eshel and Farrell, 2000), which document a direct linkage between North Atlantic climate variability and hydroclimatic shifts in the Eastern Mediterranean ideal to study past global climate changes. Second, since Lake Van is endorheic, its water level directly reflects the precipitation to evaporation ratio (Litt et al., 2009; Randlett et al., 2017). Finally, the recovered 220 m long sediment record from Ahlat Ridge is exceptionally well dated and spans the last 600 ka, corresponding to the last 15 marine isotope stages (MIS1-15; Litt et al., 2014a; Stockhecke et al., 2014a).

Previous work on the Lake Van ICDP cores has focused on the last 100 kyrs at high resolution, including precise sediment descriptions (Stockhecke et al., 2014b), pollen analysis (Litt et al., 2014a) and isotopic measurements on carbonates (Kwiecien et al., 2014). Those studies indicated cold and dry glacial periods and wet and warm interglacial periods. A high-resolution hydroclimatic reconstruction based on geochemical and color data, in agreement with a transient model, revealed that the hydrological changes recorded in the sediments are mainly controlled by the Atlantic Meridional Overturning Circulation (AMOC; Stockhecke et al., 2016). To better understand the organic carbon signal in the sediments, Randlett et al. (2014, 2017) measured source-specific biomarker abundances, i.e., long-chain *n*-alkanes produced by land-derived vegetation, and long-chain alkenones (LCAs) from aquatic algae. These biomarker abundance data, along with measurements of their hydrogen isotopic compositions (δ^2H), revealed a dry period between 110 and 10 ka. Whereas the earlier study focused on the last interglacial/glacial cycle, the current study focuses on the preceding interglacial/glacial cycle (MIS7/MIS6).

In this paper, we used source-specific biomarkers (i.e., long chain *n*-alkanes, LCAs and sterols, produced by land-derived vegetation and algae, respectively) to illuminate

paleoenvironmental changes. Those changes include aquatic productivity in the lake, vegetation in the catchment, lake level and salinity changes. Additionally, we measured δ^2H values of long-chain *n*-alkanes to reconstruct paleohydrological variations such as changes in precipitation, evaporation, and water sources during MIS7 and MIS6. We focus on this penultimate interglacial/glacial cycle (from 250 ka to 130 ka) since this time period is poorly studied, not only around Lake Van, but also globally (Cheng et al., 2006), and the Lake Van sediment record presents a unique opportunity to provide new insight on this enigmatic time period from a climatically important region.

2. Setting

Defined as a soda lake, Lake Van (38°N, 43°E, 1650 m a.s.l., Fig. 1A) water is highly alkaline (pH of 9.8) and saline (psu 19-22) (Reimer et al., 2009; Tomonaga et al., 2017). It has a volume of 607 km^3 and a maximal water depth of 460 m. Since Lake Van has no outflow, its water level directly reflects the ratio between freshwater input and evaporation, both of which are ultimately controlled by the Subtropical High Pressure Belt and mid-latitude westerly winds. In the Lake Van catchment, precipitation and river discharges are estimated at 2 to 4 $km^3\ a^{-1}$ and evaporation at approximately 4 $km^3\ a^{-1}$ (Degens et al., 1978; Reimer et al., 2009).

The local climate can be defined as continental with dry summers and precipitation mainly occurring in spring, autumn and winter (van Zeist et al., 1978). Maximum air temperatures of approximately 20°C occur between July and September (Fig. 1B). Details of meteorological data including temperatures, amount and δ^2H values of precipitation ($\delta^2H_{precipitation}$) are available for Erzurum (39°54'N, 41°16'E, 1758 m a.s.l.) and Senyurt (40.20°N, 41.50°E, 2210 m a.s.l., IAEA/WMO, 2014). Maximum precipitation of 75 mm $month^{-1}$ falls in late spring/autumn (Fig. 1C) and $\delta^2H_{precipitation}$ values show a seasonal variability of 120 ‰ (IAEA/WMO 2014). Randlett et al. (2017) identified a correlation between $\delta^2H_{precipitation}$ and air temperatures, with higher $\delta^2H_{precipitation}$ values corresponding to warmer temperatures (IAEA/WMO 2014).

The Lake Van catchment covers a surface of 16 000 km^2 (Degens and Kurtman, 1978). A strong gradient of annual precipitation is observed in this area. The southwestern region receives on average 600-800 mm precipitation, whereas the Northeast receives only half of this amount (van Zeist et al., 1978). This directly influences the type of vegetation: in the southwestern region, a Kurdo-Zagrosian oak forest is present whereas the northeastern region is characterized by remnants of an oak forest related to the high altitude plateau steppe (van Zeist et al., 1978; Wick et al., 2003).

3. Methods

3.1. Chronology and sediment samples

In 2010 the ICDP retrieved a long sediment core from Ahlat Ridge (AR; 38°40'N-42°40'E) at 350 m water depth (Fig. 1E; Litt et al., 2014b). A precise depth-age model was built using climatostratigraphic alignment, varve chronology, tephrostratigraphy, argon-argon single-crystal dating, radiocarbon dating, magnetostratigraphy and cosmogenic nuclides (Stockhecke et al., 2014a; 2016). The composite sedimentary profile of Lake Van spans the last 600 ka, corresponding to MIS1 to 15 (Stockhecke et al., 2014a). All chronological data from Lake Van, including the age model, are illustrated and published in Stockhecke et al. (2016). The age model was confirmed recently with new $^{40}Ar/^{39}Ar$ measurements on tephra from 133 ka to 251 ka revealing consistent inverse isochronal ages of five volcanoclastic layers (V-81, V-111, V-145, V-149 and V-185; Engelhardt et al., 2017).

3.2. Lipids

For lipid analyses, 103 sediment samples were selected at a millennial time scale, focusing on the penultimate interglacial/glacial cycle from 250 ka to 130 ka. Sediment was freeze-dried, homogenized, and an internal standard mix (5α-cholestane, 3-eicosanone, and *n*-C_{19}-ol) was added for biomarker quantification. Total lipids were extracted from Lake Van sediment using a SOLVpro Microwave Reaction System (Anton Paar, Graz, Austria) and a mixture of dichloromethane (DCM)/methanol (MeOH; 15 mL; 7:3 v/v) during a run of 5 minutes at 70°C (plus 2 minutes of heating up to 70°C). The total lipid extract (TLE) was isolated from the sediments by centrifugation. Salts were removed from the TLE in a separation funnel containing 20 mL of a 5 % sodium chloride (NaCl) solution. The salt free extract was extracted from this solution with 3 x 10 mL DCM. The TLE was saponified with 3 mL of 1 N KOH in MeOH at 80°C for 3 hours. At the end of the reaction, 2 mL of solvent-extracted nanopure H_2O was added to stop the reaction. The neutral lipids were extracted by liquid-liquid extraction using 3 x 1 mL of hexane (Hex). They were further separated by solid phase extraction, using 500 mg/6 mL Isolute Si gel columns (Biotage, Uppsala, Sweden). Four different fractions of increasing polarity were prepared. The first fraction contained the *n*-alkanes, eluted with 4 mL Hex; the second fraction contained the long chain alkenones (LCAs) eluted with 4 mL of 1:2 (v/v) Hex/DCM; the third fraction contained the sterols recovered with 4 mL of 95:5 (DCM:MeOH) and the last fraction with the remaining polar compounds were eluted with 4 mL MeOH. The LCA fraction was treated using a silica gel impregnated with silver nitrate, according to the protocol of d'Andrea et al. (2007). This additional separation was necessary for a robust identification and quantification of the LCAs. Nevertheless, this treatment might have led to higher uncertainties in concentration measurements, although recoveries were between 87 and 100 percent.

3.3. *n*-Alkanes, LCA, and Sterols

n-Alkanes, LCA, and sterols were identified by gas chromatography-mass spectrometry (GCMS-QP2010 Ultra, Shimadzu) and an external standard containing C_{14} to C_{40} *n*-alkanes (Sigma-Aldrich). Compounds were injected using an AOC-20i autosampler (Shimadzu) through a split/splitless injector operated in splitless mode at 280°C. The GC column, an InertCap 5MS/NP (0.25 mm x 30 m x 0.25 µm; GL Sciences, Japan) was heated from 70°C to 130°C at 20°C/min and further to 320°C at 4°C/min (20 min hold) for *n*-alkanes and sterols. LCA were run on an Agilent VF-200MS column (0.25 mm x 60 m x 0.10 µm) and the oven was heated from 50°C (held for 1 min) to 255°C at 20°C/min, to 300°C at 3°C/min, and then to 320°C at 10°C/min (held for 10 min, Longo et al., 2013). Once compounds were identified, they were quantified by gas chromatography coupled with a flame ionization detector (GC-2010 Plus, Shimadzu, Kyoto, Japan) under the same analytical conditions. Compound abundances were quantified using peak areas relative to those of the respective internal standard (5α-cholestane for *n*-alkanes, 3-eicosanone for alkenones, and C_{19} *n*-alkanol for sterols).

3.5. δ^2H and $\delta^{13}C$ measurements

$\delta^{13}C$ and δ^2H values from long-chain *n*-alkanes (from *n*-C_{25} to *n*-C_{33}) were measured in duplicate, using a Trace GC-Ultra gas chromatograph attached to a Thermo Fischer Delta-V isotope ratio mass spectrometer (irMS) via a combustion/reduction and pyrolysis interface, respectively (GC Isolink, Thermo Fischer). The GC coupled to the irMS was equipped with a 30 m DB-5MS fused silica capillary column (i.d. 0.25 mm; 0.25 µm film thickness). The oven temperature was programmed from 70°C to 300°C at a rate of 4°C/min, followed by an isothermal period of 15 min. Helium was used as a carrier gas. The samples were injected in splitless mode at 275°C. Raw isotope values were initially converted to the international standard VSMOW scale (hydrogen) and VPDB (carbon) using Thermo Isodat 3.0 software and pulses of a reference gas that was measured at the beginning and end of each analysis. Sample δ^2H values were further normalized using known values of *n*-alkane standard mixes, which were run at the beginning and end of each sequence, as well as after every 6 to 8 injections. This standard of *n*-alkanes (*n*-C_{17}, *n*-C_{19}, *n*-C_{21}, *n*-C_{23}, and *n*-C_{25}) from Arndt Schimmelmann (Indiana University) with known isotopic composition was analysed daily prior to each sample batch in order to monitor the system performance. Analytical reproducibility was 0.2 ‰ for $\delta^{13}C$ and 2-3 ‰ for δ^2H. The C_{29} *n*-alkane had the highest median concentration in all the samples; hence we show δ^2H values only for this compound.

4. Results

4.1. Organic carbon and nitrogen concentrations

Total organic carbon concentrations varied between 0.1 and 2.6% in sediments deposited during MIS7 and MIS6 (Fig. 2; Stockhecke et al., 2014b). Highest values were detected between 240-231 and 222-210 ka in MIS7, and between 200-185 ka in the transition from MIS7 to MIS6. However, we also found some single spikes with higher concentrations at 172 and 176 ka. Very low concentrations were found around 228 ka and 135-142 ka. TOC concentrations increased towards the transition to MIS5.

4.2 C/N ratio

C/N ratios (total organic carbon/total nitrogen weight ratios) were calculated from previous data (Stockhecke et al. 2014b). It varied between 5.4 and 35.7 with an average of 12.6 indicating a huge and dynamic range between autochthonous and allochthonous organic material in Lake Van sediments (Fig. 2). There was usually no strong correlation observed between TOC and C/N values, but around 240 and 230 ka and between 220 and 205 ka higher TOC values coincide with higher C/N values.

4.3. Land-derived biomarkers

Long chain *n*-alkanes (*n*-C_{27}+ *n*-C_{29}+ *n*-C_{31}) were measured as indicators for land-derived input to Lake Van sediments. Concentrations varied between 12 and 307 µg/g sediment with higher values except for some single spikes found only between 250 and 236 ka (Fig. 2). Additionally, the average chain lengths (ACL) and carbon preference index (CPI) were calculated.

ACL values defined as ACL = Σ (C_n x n)/ Σ (C_n) (chain lengths of 21 to 33 were used in this study), as a tool for characterizing the source of long-chain *n*-alkanes. Longer chain lengths (from *n*-C_{27} to *n*-C_{33}) are generally produced by land-derived vegetation, whereas intermediate chain lengths (from *n*-C_{23} to *n*-C_{25}) are present in aquatic plants (Meyers, 2003). In Lake Van sediments, ACL showed stable values around 28 to 29 that are typical for land-derived vegetation (Meyers, 2003) from 250 to 220 ka (Fig. 2). Then, ACL dropped to 25 between 218 and 210 ka. After a short increase to 28, values dropped again at 198 ka and stayed low interrupted only by two higher values between 193 and 191 ka before reaching finally values up to 29 from 175 to 130 ka.

P_{aq} is defined as P_{aq} = (*n*-C_{23}+*n*-C_{25})/(*n*-C_{23}+*n*-C_{25}+*n*-C_{29}+*n*-C_{31}) and was introduced by Ficken et al. (2000). Five main peaks higher than 0.4 were identified from 242 to 230 ka, from 220 to 208 ka, from 200 to 192 ka, from 190 to 180 ka and at 170 ka (Fig. 2). Except for those peaks, P_{aq} stayed at values around 0.2 (Fig. 2).

The CPI, first proposed by Bray and Evans, (1961), is defined as CPI = [Σ_{odd} (C_{21-33}) + Σ_{odd} (C_{23-35})]/ (2*Σ_{even} C_{22-34}) and is used as a degradation index. More specifically, a CPI>1 reflecting a predominance of odd over even chain length *n*-alkanes, indicates a land-derived plant source and thermal immaturity of the source rock (Bray and Evans, 1961). In contrast, low CPI values (around 1) reflect degraded OM, potentially related to significant bacterial activity (Chaffee et al., 1986; Stefanova et al., 1995). Through the investigated period, the average CPI was around 8 with variations between 3 and 12. These high values throughout the whole core interval reveal a good preservation of organic material and a low degradation of these biomarkers over the last 250 ka. It should be noted that the CPI followed the variations of ACL and Paq that is interpreted as a combination of higher aquatic plant input and variation in degradation.

We measured δ^2H values on long-chain *n*-alkanes (*n*-C_{25}; *n*-C_{27}; *n*-C_{29}; *n*-C_{31} and *n*-C_{33}) produced by land-derived vegetation. δ^2H values of *n*-C_{25}, *n*-C_{27}, *n*-C_{29}, *n*-C_{31} and *n*-C_{33} alkanes were highly correlated (Spearman test; rho=0.78; p value=2.10^{-16}). Since *n*-C_{29} was the most concentrated long-chain *n*-alkane in all Lake Van sediment samples, we only show δ^2H variations for this *n*-alkane (Fig. 3A). δ^2H values over the whole investigated timescale varied from -164 to -182‰, similar to the range measured in a much lower resolution from 130 to 600 ka (Randlett et al., 2017). δ^2H values were more stable in MIS6 compared to MIS7, when higher fluctuations occurred. In MIS7 between 235 and 232 ka and between 220 and 210 ka, lighter values were measured (Fig. 3A).

Over MIS7 and MIS6 $\delta^{13}C$ values of *n*-C_{29} generally fluctuated vary little: between -29.7 and 31.4‰ in MIS7 and on average a little lower between -30.2 and -31.4‰ during MIS6 (Fig. 3B).

4.4. Aquatic biomarkers

Concentrations of source-specific biomarkers produced by aquatic algae were determined with a focus on short chain *n*-alkanes (*n*-C_{15}+ *n*-C_{17}+ *n*-C_{19}) (Meyers, 2003), brassicasterol (24-methyl cholest-5,22-dien-3β-ol) mainly produced by diatoms (Volkman, 1986; 2016), dinosterol (4α,23,24-trimethyl-5α-cholest-22E-en-3β-ol) mainly produced by dinoflagellates (Whiters, 1983), and alkenones (ketones with 37 or more carbon atoms) produced by haptophytes (Brassell et al., 1986). Short chain *n*-alkane concentrations varied between 1 and a maximum of 148 µg/g sediment with higher values from 244 to 236 ka and between 190 and 184 ka (Fig. 2). A major peak of brassicasterol was measured around 235 ka (180 µg/g) at the beginning of MIS7, at a time when North et al. (2017) also measured high diatom concentrations in the sediments. The second highest concentrations of brassicasterol were recorded at the end of MIS6 and beginning of MIS5 (around 135-130 ka), reaching a maximum value of 46 µg/g. Higher concentrations around 10 µg/g were measured around 228

ka, 203 ka, 169 ka and from approximately 161 ka to 147 ka as well. Other than from these intervals, brassicasterol concentrations were at or below the detection limit (Fig. 2).

In addition to brassicasterol we also quantified dinosterol, primarily attributed to dinoflagellates, but also occurring to a limited extent in other phytoplankton like diatoms (Whiters, 1983, Volkman et al., 1993). Dinosterol was much less abundant than brassicasterol or alkenones (and detected only in 40 samples) with values well below 20 µg/g and only some higher values up to 160 µg/g at 220, 200, 160 and 134 ka (Fig. 2). Dinosterol mainly occurred at depths where brassicasterol was also abundant, indicating that both likely originated from diatoms or that dinoflagellate and diatom blooms occurred at the same time.

LCAs are exclusively produced by haptophytes, and represent another family of biomarkers considered to reflect aquatic productivity in Lake Van waters (Fig. 2). C_{37} to C_{40} alkenones were identified in Lake Van sediments: $MeC_{37:4}$, $MeC_{37:3}$, $MeC_{37:2}$, $MeC_{38:5}$, $MeC_{38:4}$, $EtC_{38:4}$, $EtC_{38:3}$, $EtC_{38:2}$, $MeC_{40:3}$, $MeC_{40:2}$ and $MeC_{40:1}$. Abundances of these compounds were correlated over the penultimate period (Spearman test; rho=0.85; $p_{value}=2.10^{-16}$), therefore only $MeC_{37:4,3,2}$ are shown (Fig. 2). $MeC_{37:4}$ and $MeC_{37:3}$ were most concentrated in Lake Van sediments. This feature is generally observed in freshwater lakes, with a predominance of $MeC_{37:4}$ alkenones (Longo et al., 2018; Song et al., 2016). Generally, MeC_{37} concentrations were higher between 250 and 230 ka (above 21 µg/g). From 250 to 240 ka, $MeC_{37:4}$ had higher concentrations. At 240 ka, a decrease of all MeC_{37} was recognized, whereas from 240 to 230 ka $MeC_{37:3}$ became more abundant (Fig. 2). This could be explained by a change of salinity (Song et al., 2016) without or with a haptophyte community change. In our case, it involves a change in haptophyte communities identified by DNA analyses taking place at the same time (Randlett et al., 2014). Indeed, before 240 ka, phylotypes closely related to *Isochrysis* and *Pseudoisochrysis* (Coolen et al., 2009) were characterized in Lake Van sediments (Randlett et al., 2014). According to Coolen et al. (2009), *Isochrysis* and *Pseudoisochrysis* mostly produce $MeC_{37:4}$. After 240 ka, another species of haptophytes was recorded but not precisely identified by Randlett et al. (2014). This species potentially produced mainly $MeC_{37:3}$ with very high values of 57 µg/g. At around 232 ka, the sum of MeC_{37} alkenone concentrations decreased to values under 1 µg/g, reaching again values of 4 µg/g at 220 ka before declining to zero around 215 ka. At 200 ka, another small rise of LCAs concentration to around 2 µg/g was detected. During MIS6, MeC_{37} alkenone concentrations were close to zero, except around 180, 170, 160 and 150 ka. At the end of MIS6 and the start of a new interglacial (MIS5) with warmer temperatures, MeC_{37} increased to 4 µg/g.

5. Discussion

5.1 Land-plant input and phytoplankton productivity in MIS7 and MIS6

TOC was much more variable during MIS7 than during MIS6, which only shows higher TOC values at the beginning of the termination and at the end towards the warmer MIS5 (Fig. 2). The bulk organic carbon composition was not consistent and showed higher C/N values, which means more land-derived OM at the first two high TOC events, whereas the last higher TOC event in MIS7 was characterized by lower land-derived input. For MIS6, higher C/N ratios were only documented at the beginning and then were in general much more stable and lower, indicating a higher aquatic OM input. Stockhecke et al. (2014b) pointed out that an increase in lake level would broaden the anoxic zone and hence would lead to a better preservation of organic carbon and higher TOC values. However, this might only partly be true since higher TOC values during some time spans in MIS7 but also in MIS6 could be explained also by an increased land-derived input. Beside C/N ratios, we measured the concentrations of long chain *n*-alkanes that are an important constituent of plant leaf waxes. With this higher plant input indicator, we see higher concentrations between 250 and 230 ka at 160 ka and around 145 ka. From all these time events, only the peak around 240 ka and around 160 ka are in line with higher TOC values. This means that other times with high TOC values were most likely influenced by a higher aquatic input. They will be discussed below.

Several researchers have calculated averaged chain lengths of *n*-alkanes to evaluate whether ACL can be an indicator for plant species or plant groups (Bush and McInerney, 2013, 2015; Ficken et al., 2000). Although early results looked promising, it is now confirmed that only Sphagnum mosses (Bush and McInerney, 2013, 2015; Ficken et al., 2000) and submerged aquatic plants (Ficken et al., 2000) with lower ACL values of around 23 and 25 carbons, can be clearly distinguished with this metric. Another indicator is called P_{aq} = (*n*-C_{23}+*n*-C_{25})/(*n*-C_{23}+*n*-C_{25}+*n*-C_{29}+*n*-C_{31}) and was proposed by Ficken et al. (2000) based also on the chain length of lipids (*n*-alkanes). Values of 0.01-0.23 should be indicative of land-derived plants, 0.07-0.61 for emerged plants, and 0.48-0.94 for submerged/floating plants. In the Lake Van sediment core, this would characterize the times between 220 and 205 ka and around 185 ka as periods with higher submerged/floating plant inputs since P_{aq} and ACL were high and low respectively. The rest of the core would be interpreted as dominated by land-derived plants. Interestingly, the two time windows with high P_{aq} and low ACL were times at which higher arboreal plant pollen were counted (Fig. 2; Litt al. 2014a). Pollen and molecular biomarkers were described to register different paleoenvironmental signals (e.g. Zhang et al., 2018). Although both reflect land-derived vegetation, pollens are easily transported over long distances by wind and accumulate in sediments, reflecting more the regional scale. In contrast, biomarkers coming mainly from leave waxes are less susceptible to long-distance aeolian

transport and provide a local picture of the land-derived vegetation (Leopold et al., 1982; Schwark et al., 2002).

High pollen abundances and high concentrations of aquatic input reflecting biomarkers could also be explained by the fact that the aquatic production was even higher than the land-derived input.

Nonetheless, also the aquatic input indicating organic compounds do not always coincide. For instance, between 240 and 234 ka and around 185 ka, short-chain *n*-alkane concentrations as an indicator for aquatic organic material were high, although no indication from Paq or ACL is given for a higher aquatic plant input between 240 and 234 ka. At 185 ka, the higher concentration of short-chain *n*-alkanes are in line with the Paq and ACL indices and might indicate an algal bloom. On the other hand, between 220 and 205 ka when Paq and ACL is indicating a higher aquatic plant input, short chain *n*-alkane concentrations stayed low (Fig. 2).

Recent research showed that ACL might be an indicator for changes in temperatures and hydrological conditions (Bush and McInerney, 2015; Hoffmann et al., 2013). Hence, in the Lake Van region, this could mean that between 220 and 205 ka and around 185 ka, average ACL values in plants living in the Lake Van catchment changed because the temperature or hydrological conditions changed significantly. Indeed, strong precipitation anomalies leading to drier and wetter conditions have been described during this time (Stockhecke et al., 2016). Bush and McInerney, (2015) showed a correlation of increased ACL with higher temperature and argued that during periods of warmer temperatures, longer chain length *n*-alkanes on leaf surfaces would be more stable. In the context of our study, we could argue that the two periods of low ACL values could be explained by a colder and drier climate, rather than a higher submerged aquatic plant input. It has, however, also been shown that different plant species react differently to hydrological changes, i.e., with either increasing or decreasing chain length (Hoffmann et al. 2013). Hence, an argument about wetter, drier or colder, warmer climate is difficult, if not impossible, to make based on ACL values alone.

To link ACL to climate despite the aforementioned difficulties, we compared ACL to a principal component analysis of sediment reflectance color, TOC, $CaCO_3$, potassium and silica contents (Stockhecke et al., 2016). Positive values of the first principal component (PC1) are associated with high reflectance color, anomalously low Si and K, high TOC and $CaCO_3$ concentrations and were interpreted as anoxic conditions due to intensified stratification, higher productivity, an increased shore-line distance by increased runoff and forested vegetation in the watershed during lake-level rises. In conclusion, all those effects were interpreted as the result of higher run-off (i.e., higher precipitation/evaporation ratios) and wetter climate (Stockhecke et al., 2016). When comparing ACL to PC1, it is evident that the two times (220 to 205 ka and around 185 ka) at which low ACL were measured, the PC1 was

also high (Fig. 2). Hence, a wetter climate could have triggered plants to build shorter chain lengths as described in Bush and McInerney (2015). Additionally, an increased lake surface due to higher run-off might also initiated a higher supply of submerged plants also leading to shorter ACL values.

Aquatic proxies covary at key time intervals in the Lake Van record. Higher LCA concentrations (i.e., higher abundance of coccolithophores, assuming LCA /coccolithophore concentrations stayed similar) occurred at the transition from MIS8 to MIS7 (Fig. 2). The same is true for brassicasterol concentrations, indicating greater diatom abundance, and both LCA and brassicasterol concentrations were high in the first wetter phase from 240 to 230 ka. This has also been recognized by counting diatoms fragments with higher abundances between 238 to 236 ka (North et al., 2017). In the following drier phase identified from PC1, both proxies showed low concentrations. This indicates that the slightly colder and drier stadial was not the preferred climate for phytoplankton growth, similar to tree pollen, which decreased dramatically during this time. Whereas the proxy for dinoflagellates was low during this time interval, it then increased at the beginning of the warmer phases at 220 and 200 ka. In this interval, brassicasterol stayed low and hence became uncoupled from the dinosterol signal. If these biomarker concentrations reflect diatom and dinoflagellate populations following the standard interpretative model, this suggests that dinoflagellate and diatom populations responded to changes at this time in different ways. Alternatively, if the dinosterol in Lake Van sediments is diatom derived, then the diatom species distribution must have changed.

During MIS6 all three indicators for phytoplankton stayed rather low with some single peaks at 170 ka (both dinosterol and brassicasterol, i.e., dinoflagellates and diatoms or diatoms producing both markers) and 155 ka (only brassicasterol which showed a similar signal as at 200 ka with different diatom species or dinoflagellates). A high brassicasterol signal then occurred at the end of MIS6, when higher TOC values also indicate higher phytoplankton productivity. Interestingly, the highest diatom peak in MIS7 around 235 ka (consistent with diatom analyses; North et al. 2017) might be related to a high input of silica at 237 to 233 ka, which was found by XRF scanning of the core (Kwiecien et al., 2014) and related to a fresh-water period (e.g., decreased diatom dissolution) and likely a hydrologically open lake system (North et al., 2017). Comparing the LCA concentrations with a temperature record from the Mediterranean Sea from 250 to 130 ka based on LCA temperature estimates (Emeis et al., 2003), it is possible to see that higher LCA concentrations in Lake Van usually occurred when temperatures in the Mediterranean were also higher. One exception is the time around 220 ka when temperatures in the Mediterranean were cold but we see the second highest LCA concentrations in Lake Van. At this time, a so-called “cold” sapropel (S8) was formed in the eastern Mediterranean and was related to a high extant of ice sheets at high latitudes (Lisiecki & Raymo, 2005). The colder climate is also seen in the pollen record, which shows very low

concentrations of arboreal pollen around 220 ka (Litt et al., 2014a). In general, with the aforementioned exception, the LCA concentration follows temperature changes in Lake Van, even if Randlett et al. (2014) showed that the numerous changes of haptophyte communities prevents an estimation of local paleotemperatures using LCAs. Overall, in MIS6 in the Lake Van area was most likely a dry and cold stage with very little phytoplankton productivity compared to MIS7, although in MIS7 we also found colder phases with no or very little phytoplankton remains in the sediments.

5.2. Paleohydrological changes during the penultimate period around Lake Van

Randlett et al. (2017) and Tomonaga et al. (2017) used source-specific markers (δ^2H on *n*-alkanes, LCAs) and pore-water salinity, respectively to reconstruct paleohydrological changes at Lake Van during the last 600 ka. However, quantitative reconstruction of pore-water salinity was only possible back to 250 ka (Tomonaga et al., 2017), and the resolution of δ^2H values on *n*-alkanes and LCAs earlier than 130 ka was very low (over the timescale investigated here only 11 values are available). Furthermore, paleoconductivity and lake-level reconstructions based on diatom species are limited to low-alkaline (high lake-level) periods due to poor frustule preservation in high-alkaline lake water (North et al., 2017). Hence, in order to extend the timespan and increase continuity of previous quantitative reconstructions of paleohydrological changes around Lake Van, we measured δ^2H on long-chain *n*-alkanes from 250 ka to 130 ka.

Before deriving any paleohydrological information from plant wax δ^2H values, it is important to exclude other factors that might influence those values. One factor that could influence the interpretation of δ^2H values from plant waxes could be the variation of vegetation, for instance, a change from C_3 plants to C_4 plants for example. Whereas *n*-alkanes from C_3 plants have $\delta^{13}C$ values around -34.7‰, C_4 plants have higher values of around -21.4‰ (Castañeda et al., 2009). $\delta^{13}C$ values of plant waxes in Lake Van sediments lie in a very small range of -29.7 and 31.4‰ indicating a C_3 dominated vegetation (Fig. 3B). Another hint could be the linear correlation between $\delta^{13}C$ and δ^2H (Fig. 3C), which could be interpreted as a stomatal constraint on leaf gas-exchange mediated by water supply rather than a change in plant type, a mechanism occurring in sub arid regions (Kahmen et al., 2013a; Kahmen et al., 2013b; Zech et al., 2015). This supports the idea that δ^2H values from plants that produced these compounds may indeed be driven primarily by water stress, and therefore that the δ^2H record over MIS7 to MIS6 can be interpreted to reflect changes in paleohydrology, i.e., the precipitation and evaporation balance.

When comparing the interglacial and glacial period, MIS7 shows a higher range and oscillation of the δ^2H values indicating a fluctuation between wetter and drier times than MIS6 during which δ^2H values stayed around -170‰ (±3‰), indicating a drier climate. In MIS7,

especially two (three) time slices between 215 to 210 ka and 197 to 185 ka (and 244 to 235 ka; not as strong) indicate a wetter climate. A climate, which was wetter in MIS7, is also supported by an increasing lake level from 470 m below present lake level in MIS8 to about only 270 m below present sea level around 230 ka (Cukur et al., 2014). Cukur et al. (2014) also identify a lake level decrease to 310 m below present lake level at MIS6, which supports our estimation that MIS6 was rather dry at Lake Van. In general, it can be concluded that the differences in climate between MIS7 and MIS6 are a drier climate in MIS6 and an overall wetter with some drier phases in MIS7, similar to MIS5. For MIS6, our data shows that it was not as dry as the timespan from 110 to 10 ka investigated on the same core (Randlett et al., 2017), when a very dry climate prevailed in the Lake Van area.

5.3. Paleohydrological changes during MIS7 and MIS6 in the Mediterranean

The underlying mechanism for the hydroclimatic changes in the Eastern Mediterranean and its relationship to Northern hemispheric ice-sheet dynamics, the Atlantic Meridional Overturning Circulation (AMOC) and reorganization of atmospheric circulation was previously scrutinized by Stockhecke et al. (2016). It was shown that cooling and aridity in the Eastern Mediterranean resulted from enhanced North Atlantic glacial iceberg calving and weaker AMOC for a period of large ice-sheets and low sea level. Increasing precession led to an enhancement of spring to early summer precipitation, as well as winter precipitation through the enhancement of the winter storm track, which caused overall increased rainfall and lake level rise during periods of small ice-sheets and high sea-level (Stockhecke et al., 2016).

To obtain a regional overview of paleohydrological changes during the penultimate interglacial/glacial we compared our Lake Van paleoclimatic/paleohydrological record, meaning the δ^2H measurements on long-chain *n*-alkanes, first to other parameters derived from Lake Van sediments like the PC1 hydroclimatic reconstruction from Stockhecke et al. (2016) and lake level reconstruction from Stockhecke et al. (2014b), and second to paleoclimatic records from around the Mediterranean and the Arabian peninsula (Fig.1D and 4). This comparison includes: (i) an East Mediterranean sapropel record (Rossignol-Stick and Paterne, 1999); (ii) speleothems from Oman (Burns et al., 2001); (iii) speleothem clusters from the Negev caves (Vaks et al., 2010), and (iv) tree pollen from North East Greece (Tzedakis et al., 2006). All records registered quite similar paleohydrological variations during the investigated period (Fig. 4).

During MIS7, three wetter episodes from 197 to 185 ka, 215 to 210 ka, and 244 to 235 ka could be identified from the hydrogen isotope profile by more negative δ^2H values of C_{29} *n*-alkanes. We observed a strong correlation to previously measured parameters from Lake Van, where wetter conditions were identified by positive values of the hydroclimatic reconstruction PC1 (Stockhecke et al., 2016). Furthermore, two of the above-mentioned periods fall into

periods when high lake water level prevailed, i.e., around 250-230 ka and 220-210 ka (Stockhecke et al., 2014b). Around those times, sapropel layers (7, 8, and 9, Langereis et al., 1997) were formed in the Mediterranean, more specifically the Tyrrhenian Sea (Emeis et al., 1991). However, the climate interpretation based on pollen from these sapropels is not the same for all three (Rossignol-Stick and Paterne, 1999). Whereas during sapropel 7 and 9, the pollen percentage of deciduous oak (*Quercus*) was high (above 30%), and that of sage-brush (*Artemisia*) was low (10%), indicating a warmer and wetter climate. During sapropel 8, the concentrations for sage-brush were high (above 60%), and for oak low (15–20%), revealing a colder and drier climate. The same pollen distribution exists in sapropel 6 (around 176 ka in MIS6) in the Mediterranean Sea. The difference in pollen distribution in the sapropels in MIS7 at the times when sapropels (7, 8, and 9) were deposited was not seen in our hydrogen isotope record, which shows rather similar values over all three time slices and hence similar conditions. An investigation about sapropel formation in the Mediterranean concluded that in general sapropels coincided with a warming trend at a regional (Emeis et al., 2003) and global scale (Lisiecki & Raymo, 2005). In this interpretive model, warming surface waters prohibited deep convection and hence anoxic water layers leading to sapropels were formed. This warming and a wetter climate are in line with δ^2H values on *n*-C_{29} alkanes at 197 to 185 ka and 244 to 235 ka. However, a colder climate as deduced from $\delta^{18}O$ values of the ice core LR04 (Lisiecki & Raymo, 2005) and from LCAs in the Mediterranean Sea (Emeis et al., 2003) cannot be seen in δ^2H values on *n*-C_{29} alkanes (which is similar) at the time when sapropel 8 (215 to 210 ka) was formed.

During the time when sapropel 6 was deposited the δ^2H values on *n*-C_{29} alkanes in Lake Van showed rather heavy values, indicating a drier and colder climate in contrast to the time when the other three sapropel layers were deposited. A colder and drier climate was also suggested in the Mediterranean for the time when sapropel 6 (“a glacial sapropel”) was deposited, although this contradicts the general feature of sapropel deposition during warmer times (Emeis et al., 2003).

In stark contrast to our findings, the Dead Sea area was characterized by wetter climate during glacial period MIS6 and drier climate during the MIS7 interglacial period (Torfstein et al., 2009; Waldmann et al., 2010). Although the main moisture source was most likely the Mediterranean Sea, additional southern sources were suggested since sporadic deposition of travertines and speleothems occurred in the Negev Desert and Arava Valley during past interglacials (Waldmann et al., 2010). On the other hand, reconstructions from sediments from the Yammouneh basin (Northern Lebanon) described a wetter early-mid interglacial MIS7 with forested areas and a drier glacial MIS6 (also getting wetter during this stage) with more open vegetation (Gasse et al., 2011) in accord with our results. This drier and colder MIS6 in the Dead Sea basin was at least confirmed from pollen analysis during the later stage (147-130

ka) of MIS6 (Chen and Litt, 2018). Hence, there are contrasting reports for the area south of Lake Van with both similar and opposing findings to those from Lake Van.

Interestingly, in the Middle East (Oman) the growth of speleothems was described for the period 200 to 180 ka, revealing wetter climate in this region (Burns et al., 2001). Further to the west in a cave in Yemen, speleothems were also found during 245 to 230 ka (Fleitmann et al., 2011). Speleothem growth was found during the so-called Negev humid period 2 (between 220 and 190 ka; Vaks et al., 2010) in the Negev desert south of the Dead Sea basin, indicating wetter conditions. All these findings record wetter conditions in the area from the Mediterranean Sea up to the Middle East. In Lake Van we clearly see also the wetter period from 245 to 230 ka found in Yemen (Fleitmann et al., 2011). Instead of the wetter period from 220 to 190 ka in the Negev desert (Vaks et al., 2010) and the coinciding wetter period in Oman from 200 to 180 ka, Lake Van shows two distinct wetter periods from 220 to 210 ka and from 195 to 185 ka, interrupted by a dry period from 210 to 195 ka. This dry period is actually one of the driest periods in MIS7 and MIS6 in the Lake Van area indicated by very heavy δ^2H values on *n*-C_{29} alkanes. A pollen record from Greece over the last 1.35 million years shows, similarly to the Lake Van δ^2H profile, a dry period between 225 and 230 ka whereas the rest of MIS7 shows a high pollen abundance interpreted as a wetter climate (Tzedakis et al., 2006). Interestingly in this pollen record, MIS6 was described as having a rather harsh climate with a strong decrease in tree abundance in comparison to other glacial periods and only MIS12 showed a stronger decline in tree abundances. This is very similar to Lake Van sediments with very little arboreal pollens in MIS6 (Litt et al., 2014a). Hence, it looks like the climate was very similar from the Mediterranean over Greece, Lake Van and further to the Middle East (Yemen/Oman), whereas reports from the Dead Sea basin either are in line with or completely oppose our findings. Findings that show opposite signals to ours in the Dead Sea Basin might be related to the fact that this area lies in the rain shadow of the Judean Mountains and hence recorded different climatic signals (Gasse et al., 2011).

5. Conclusion

In order to understand paleoenvironmental and climatic changes during the second to last interglacial/glacial cycle (MIS7 and MIS6) in the Near East, we quantified source-specific biomarkers in sediments of Lake Van. To quantify the input of land-derived organic material we measured the concentration of long-chain *n*-alkanes (*n*-C_{27} to *n*-C_{31}), whereas for organic material originating from autochthonous source we measured the concentration of long-chain ketones (LCAs) and sterols, representing different algae classes. Additionally, we determined δ^2H values of the long-chain *n*-C_{29} alkane to reveal information about precipitation and/or evaporation. The glacial period MIS6 was generally drier and colder and the interglacial period MIS7 wetter and warmer around Lake Van. During MIS7, the δ^2H values of *n*-C_{29} alkanes

indicated a climatically unstable period with warmer and wetter periods interrupted by cooler and drier episodes. During warmer and wetter intervals of the penultimate interglacial, a higher input of aquatic organic matter to Lake Van sediment was recorded by higher concentrations of LCAs and brassicasterol (indicating haptophytes and diatoms, respectively). The highest input of diatoms around 235 ka may be related to freshening of the lake water and high run-off that delivered silicate as a substrate for diatom growth and allowed their preservation in Lake Van. During the first wetter period (242 to 235 ka), the input of land-derived organic material (long-chain *n*-alkanes) was also higher.

In general, in accordance with other studies, it looks like the climate has been very similar from the Mediterranean to Northern Greece, the Lake Van area and further to the Middle East (Yemen/Oman) during MIS7 and MIS6. A comparison with MIS5 to MIS2, showed that the extremely arid period recorded between 110 and 10 kyrs (Randlett et al., 2017) was an exceptional event registered around Lake Van over the last 245 ka, not seen during MIS6 or MIS7.

Acknowledgements

We thank the PALEOVAN team for support during collection and sharing of data. We also would like to thank Serge Robert for his help in the laboratory. Finally, we are grateful to Jeroen Van der Wildenberg and Jean-Philippe Crettaz for their help with lipid extraction and separation.

The authors acknowledge funding from the Swiss National Science Foundation (SNF) 200021_124981, 200020_143330, P300P2-158501 200020_143340, 20FI21_124972, 200021_124981, and 200020L_156110 / 1, the PALEOVAN drilling campaign by the International Continental Scientific Drilling Program (ICDP), the Deutsche Forschungsgemeinschaft (DFG) LI 582/20-1, the Scientific and Technological Research Council of Turkey (Tübitak) and the Austrian Science Foundation (FWF Project No. I 2068-N29).

Figure captions

Figure 1: A) Bathymetry map and surrounding of Lake Van. (B) Annual temperature (°C) and (C) precipitation (mm/month) recorded in Erzurum and Senyurt around Lake Van (IAEA/WMO 2014). D) Locations of climate reconstruction records in the Eastern Mediterranean region.

Figure 2: Profile of TOC (%, Stockhecke et al. 2014b), C/N ratios, sum of long-chain *n*-alkanes (µg/g sediment), sum of short-chain *n*-alkanes (µg/g sediment), average chain length of n-alkanes (ACL), Paq, the arboreal pollen record from Litt et al. (2014a), concentrations of brassicasterol (µg/g sediment), dinosterol (µg/g sediment), alkenones (µg/g sediment), and the hydroclimatic record (PC1) from Stockhecke et al. (2016).

Figure 3: $\delta^{2}H$ and $\delta^{13}C$ values of the long-chain *n*-alkane C_{29} and the correlation between both parameters.

Figure 4: Records of climate reconstructions globally and in the Eastern Mediterranean:$\delta^{18}O$ of the ice core LR04 (Lisiecki & Raymo, 2005) with the difference between June and December insolation at 39°N (Laskar et al., 2004), a regional temperature record from the East Mediterranean Sea (Emeis et al., 2003), sapropels identified in the East Mediterranean (Rossignol-Strick and Paterne, 1999), speleothems recorded from Oman (Buns et al., 2001), percentage of tree pollen quantified from the Philippion basin in Greece (Tzedakis et al., 2006), speleothem clusters found in Negev Caves (Vaks et al., 2007), periods of high lake-water levels defined by Stockhecke et al. (2014), PC1 a paleohydrological reconstruction modeled by Stockhecke et al. (2016), and the $\delta^{2}H$ values of the long-chain *n*-alkane C_{29} from this study.

References

Barker, S., Knorr, G., Edwars, R.L., Parrenin, F., Putnam, A.E., Skinner, L.C., Wolff, E., Ziegler, M., 2011. 800,000 years of abrupt climate variability. Science 334, 347-351.

Brassell, S.C., Brereton, R.G., Eglinton, G., Grimalt, J., Liebezeit, G., Marlowe, I.T., Pflaumann, U., Sarnthein, M. (1986). Palaeoclimatic signals recognized by chemometric treatment of molecular stratigraphic data. Organic Geochemistry 11: 649-660.

Bray, E.E., and Evans E.D., 1961. Distribution of n-paraffins as a clue to recognition of source beds. Geochimica et Cosmochimica Acta 22, 2-15.

Bush, R.T., McInerney, F.A., 2013. Leaf wax n-alkane distributions in and across modern plants: Implications for paleoecology and chemotaxonomy. Geochimica et Cosmochimica Acta 117, 161-179.

Bush, R.T., McInerney, F.A., 2015. Influence of temperature and C4 abundance on n-alkane chain length distributions across the central USA. Organic Geochemistry 79, 65-73.

Burns, S. J., Fleitmann, D., Matter, A., Neff, U., Mangini, A., 2001. Speleothem evidence from Oman for continental pluvial events during interglacial periods. Geology 29 (7), 623-626.

Castañeda, I.S., Mulitza, S., Schefuß, E., Lopes dos Santos, R.A., Sinninghe Damste, J.S., Schouten, S., 2009. Wet phases in the Sahara/ Sahel region and human migration patterns in North Africa, Sahel region and human migration patterns in North Africa, Proc. Natl. Acad. Sci. U. S. A., 106, 20159e20163.

Chaffee, A.L., Hoover, D.S., Johns, R.B., Schweighardt, F.K., 1986. Biological markers extractable from coals**.** R.B. Johns (Ed.), Biological Markers in the Sedimentary Record, Elsevier, New York (1986), 311-345.

Cheng, H., Edwards, L., Wang, Y., Kong, X., Ming, Y., Kelly, M.J., Wng, X., Gallup, C.D., 2006. A penultimate glacial monsoon record from Hulu Cave and two-phase glacial terminations. Geology 34 (3), 217-220.

Chen, C., Litt, T., 2018. Dead Sea pollen provides new insights into the paleoenvironment of the southern Levant during MIS 6–5. Quaternary Science Reviews 188, 15-27.

Cukur, D., Krastel, S., Schmincke, H.U., Sumita, M., Tomonaga, Y., Namık Çağatay, M., 2014. Water level changes in Lake Van, Turkey, during the past ca. 600 ka: climatic, volcanic and tectonic controls. Journal of Paleolimnology 52, 201-214.

D'Andrea W.J., Liu Z., Da Rosa Alexandre M., Wattley S., Herbert T.D. and Huang Y., 2007. An efficient method for isolating individual long-chain alkenones for compound-specific hydrogen isotope analysis. Analytical Chemistry 79, 3430–3435.

Degens, E.T., Kurtman, F., 1978. The Geology of Lake Van. Ankara, MTA Press.

638 Djamali, M., de Beaulieu, J.-L., Shah-hosseini, M., Andrieu-Ponel, V., Ponel, P., Amini, A.,
639 Akhani, H., Leroy, S.A.G., Stevens, L., Lahijani, H., Brewer, S., 2008. A late Pleistocene
640 long pollen record from Lake Urmia, NW Iran. Quaternary Research 69, 413-420.
641 Emeis, K.C., Schulz, H., Struck, U., Rossignol-Strick, M., Erlenkeuser, H., Howell, M.W.,
642 Kroon, D., Mackensen, A., Ishizuka, S., Oba, T., Sakamoto, T., Koizumi, I., 2003.
643 Eastern Mediterranean surface water temperatures and $\delta^{18}O$ during deposition of
644 sapropels in the late Quaternary. Paleoceanography, 18, 1005,
645 doi:10.1029/2000PA000617.
646 Engelhardt, J.F., Sudo, M., Stockhecke, M., Oberhänsli, R., 2017. Feldspar $^{40}Ar/^{39}Ar$ dating of
647 ICDP Paleovan cores. Geochimica et Cosmochimica Acta 217, 144-170.
648 Ficken, K.J., Li, B., Swain, D.L., Eglinton, G., 2000. An n-alkane proxy for the sedimentary
649 input of submerged/floating freshwater aquatic macrophytes. Organic Geochemistry
650 31, 745-749.
651 Gasse, F., Vidal, L., Develle, A.-L., Van Campo, E., 2011. Hydrological variability in the
652 Northern Levant: a 250 ka multiproxy record from the Yammouneh (Lebanon)
653 sedimentary sequence. Climate of the Past 7(4): 1261-1284.
654 Hoffmann, B., Kahmen, A., Cernusak, L.A., Arndt, S.K., Sachse, D., 2013. Abundance and
655 distribution of leaf wax n-alkanes in leaves of Acacia and Eucalyptus trees along a
656 strong humidity gradient in northern Australia. Organic Geochemistry 62, 62-67.
657 IAEA/WMO, 2014. Global network of isotopes in precipitation. The GNIP Database (locations:
658 Erzurum, Senyurt).
659 Kasper, S., van der Meer, M.T.J., Mets, A., Sinninghe Damsté, J.S., Schouten, S., 2014.
660 Salinity changes in the Agulhas leakage area recorded by stable hydrogen isotopes of
661 C37 alkenones during Termination I and II. Climate of the Past 10, 251-260.
662 Kwiecien, O., Stockhecke, M., Pickarski, N., Heumann, G., Litt, T., Sturm, M., Anselmetti, F.,
663 Kipfer, R., Haug, G.H., 2014. Dynamics of the last four glacial terminations recorded in
664 Lake Van, Turkey. Quaternary Science Review 104: 42-52.
665 Ladd, S.N., Dubois, N., Schubert, C., 2017. Interplay of temperature, productivity, and
666 community assemblage on hydrogen isotope signatures of algal lipid biomarkers.
667 Biogeosciences discussions, 1-31, doi:10.5194/bg-2017-60, 2017.
668 Langereis, C.G., Dekkers, M.J., de Lange, G.J., Paterne, M., van Sandvoort, P.J.M., 1997.
669 Magnetostratigraphy and astronomical calibration of the last 1.1 Myr from an
670 easternMediterranean piston core and dating of short events in the Brunhes. Geophys.
671 J. Int. 129, 75–94.
672 Laskar, J., Robutel, P., Joutel, F., Gastineau, M., Correis, A.C.M., Levrard, B., 2004. A long
673 term numerical solution for the insolation quantities of the Earth. Astronomy and
674 Astrophysics 428, 261-285.

675 Leopold, E.B., Nickmann, R., Hedges, J.I., Ertel, J.R., 1982. Pollen and lignin records of late
676 quaternary vegetation, lake Washington. Science 218, 1305-1307.
677 Lisiecki, L.E., Raymo, M.E., 2005. A Pliocene-Pleistocene stack of 57 globally distributed
678 bentic $\delta^{18}O$ records. Paleoceanography 20, PA1003.
679 Litt, T., Krastel, S., Sturm, M., Kipfer, R., Orcen, S., Heumann, G., Franz, S.O., Ülgen, U.B.,
680 Niessen, F., 2009. "PALEOVAN, International Continental Scientific Drilling Program
681 (ICDP): site survey results and perspectives." Quaternary Science Reviews 28(15-16):
682 1555-1567.
683 Litt, T., Pickarski, N., Heumann, G., Stockhecke, M., Tzedakis, P.C., 2014a. A 600,000 years
684 long continental pollen record from Lake Van, Eastern Anatolia (Turkey). Quaternary
685 Science Reviews 104: 30-41.
686 Litt, T. and Anselmetti, F.S., 2014b. Lake Van deep drilling project PALEOVAN. Quaternary
687 Science Reviews 104: 1-7.
688 Longo, W.M., Dillon, J.T., Tarozo, R., Salacup, J.M., Huang, Y., 2013. Unprecedented
689 separation of long chain alkenones from gas chromatography with a
690 poly(trifluoropropylmethylsiloxane) stationary phase. Organic Geochemistry 65, 94–
691 102.
692 Longo, W.M., Huang, Y., Yao, Y., Zhao, J., Giblin, A.E., Wang, X., Zech, R., Haberzetti, T.,
693 Jardillier, L., Toney, J., Liu, Z., Krivonogov, S., Chu, G., D'Andrea, W.J., Harada, N.,
694 Nagashima, K., Sato, M., Yonenobu, H., Yamada, K., Gotanda, K., Shinozuka, Y.,
695 2018. Widespread occurrence of distinct alkenones from Group I haptophytes in
696 freshwater lakes: Implications for paleotemperature and paleoenvironmental
697 reconstructions. Earth and Planetary Sciences 492, 239-250.
698 Meyers, P.A., 2003. Applications of organic geochemistry to paleolimnological reconstructions:
699 a summary of examples from the Laurentian Great Lakes. Organic Geochemistry 34,
700 261–289.
701 North, S.M., Stockhecke, M., Tomonoga, Y., Mackay, A.W., 2017. Analysis of a fragmentary
702 diatom record from Lake Van (Turkey) reveals substantial lake-level variability during
703 previous interglacials MIS7 and MIS5e. Journal of Paleolimnology 59, 119-133.
704 Pickarski, N., Litt , T., 2017. A new high-resolution pollen sequence at Lake Van, Turkey:
705 insights into penultimate interglacial-glacial climate change on vegetation history.
706 Climate of the Past 13, 689-710.
707 Randlett, M.-E., Coolen, M.J.L., Stockhecke, M., Pickarski, N., Litt, T., Balkema, C., Kwiecien,
708 O., Tomonaga, Y., Wehrli, B., Schubert, C.J., 2014. Alkenone distribution in Lake Van
709 sediment over the last 270 ka: influence of temperature and haptophyte species
710 composition. Quaternary Science Reviews 104, 53-62.

711 Randlett, M.-E., Bechtel, A., van der Meer, M.T.J., Peterse, F., Litt, T., Pickarski, N., Kwiecien,
712 O., Stockhecke, M., Wehrli, B., Schubert, C.J., 2017. Biomarkers in Lake Van
713 sediments reveal dry conditions in Eastern Anatolia during 110.000-10.000 years B.P.
714 Geochemistry, Geophysics, Geosystems 18, 571-583.
715 Reimer, A., G. Landmann, Kempe, S., 2009. Lake Van, Eastern Anatolia, Hydrochemistry and
716 History. Aquatic Geochemistry 15(1): 195-222.
717 Rossignol-Strick, M., Paterne, M., 1999. A synthetic pollen record of the eastern Mediterranean
718 sapropels of the last 1 Ma: implications for the time-scale and formation of sapropels.
719 Marine Geology 153, 221-237.
720 Sachse, D., Billault, I., Bowen, G.J., Chikaraishi, Y., Dawson, T.E., Feakins, S.J., Freeman,
721 K.H., Magill, C.R., McInerney, F.A., van der Meer M.T.J., Polissar, P., Robins, R.J.,
722 Sachs, J., Schmidt, H-L., Sessions, A.L., White, J.W.C., West, J.B., Kahmen, A., 2012.
723 Molecular paleohydrology: interpreting the Hydrogen-isotopic composition of lipid
724 biomarkers from photosynthesizing organisms. Annual Review of Earth and Planetary
725 Sciences 40(1): 221-249.
726 Schwark, L., Zink, K., Lechterbeck, J., 2002. Reconstruction of postglacial to Holocene
727 vegetation history in terrestrial Central Europe via cuticular lipid biomarkers and pollen
728 records from lake sediments. Geology 30, 463-466.
729 Stefanova, M., Magnier, C., Velinova, D., 1995. Biomarker assemblage of some Miocene-aged
730 Bulgarian lignite lithotypes. Organic Geochemistry 23, 1067–1084.
731 Stockhecke, M., Kwiecien, O., Vigliotti, L., Anselmetti, F.S., Beer, J., Cagatay, M.N., Channell,
732 J.E.T., Kipfer, R., Lachner, J., Litt, T., Pickarski, N., Sturm, M., 2014a.
733 Chronostratigraphy of the 600 ka old continental record of Lake Van (Turkey).
734 Quaternary Science Reviews 104: 8-17.
735 Stockhecke, M., Sturm, M., Brunner, I., Schmincke, H-U., Sumita, M., Kipfer, R., Cukur, D.,
736 Kwiecien, O., Anselmetti, F.S., 2014a. Sedimentary evolution and environmental
737 history of Lake Van (Turkey) over the past 600, 000 years. Sedimentology 61(6): 1830-
738 1861.
739 Stockhecke, M., Timmermann, A., Kipfer, R., Haug, G.H., Kwiecien, O., Friedrich, T., Menviel,
740 L., Litt, T., Pickarski, N., Anselmetti, F., 2016. Millennial to orbital-scale variations of
741 drought intensity in the Eastern Mediterranean. Quaternary Science Reviews 133, 77-
742 95.
743 Svensson, A., Andersen, K.K., Bigler, M., Clausen, H.B., Dahl-Jensen, D., Davies, S.M.,
744 Johnsen, S.J., Muscheler, R., Parrenin, F., Rasmussen, S.O., Reothlisberger, R.,
745 Seierstad, I., Steffensen, J.P., Vinther, B.M., 2008. A 60000 year Greenland
746 stratigraphic ice core chronology. Climate of the Past, 4, 47–57.

747 Tomonaga, Y., Brennwald, M.S., Livingstone, D.M., Kwiecien, O., Randlett, M-E., Stockhecke,
748 M., Unwin, K., Anselmetti, F.S., Beer, J., Haug, G.H., Schubert, C., Sturm, M., Kipfer,
749 R., 2017. Porewater salinity reveals past lake-level changes in Lake Van, the Earth's
750 largest soda lake. Scientific Reports 7: 313, 1-10.
751 Torfstein, A., Haase-Schramm, A., Waldmann, N., Kolodny, Y., Stein, M., 2009. U-series and
752 oxygen isotope chronology of the mid-Pleistocene Lake Amora (Dead Sea basin).
753 Geochimica et Cosmochimica Acta 73, 2603-2630.
754 Tzedakis, P.C, Hooghiemstra, H., Pälike, H., 2006. The last 1.35 million years at Tenaghi
755 Philippon: revised chronostratigraphy and long-term vegetation trends. Quaternary
756 Science Reviews 25, 3416-3430.
757 Vaks, A., Bar-Matthews, A., Matthews, A., Ayalon, M., Frumkin, A., 2010. Middle-Late
758 Quaternary paleoclimate of northern margins of the Saharan-Arabian Desert:
759 reconstruction from speleothems of Negev Desert, Israel. Quaternary Science Reviews
760 29, 2647-2662.
761 Vasiliev, I., Mezger, E.M., Lugli, S., Reichart, G.-J., Manzi, V., Roveri, M., 2017. How dry was
762 the Mediterranean during the Messinian salinity crisis? Palaeogeography,
763 Palaeoclimatology, Palaecology 471; 120-133.
764 van Zeist, W., Woldring, H., 1978. A postglacial pollen diagram from Lake Van in east Anatolia.
765 Review of Palaeobotany and Palynology 26(1–4): 249-276.
766 Volkman J.K., 1986. A review of sterol markers for marine and terrigenous organic matter.
767 Organic Geochemistry 9: 83–100.
768 Volkman J.K., 2016. Sterols in Microalgae. M.A. Borowitzka et al. (eds.), The Physiology of
769 Microalgae, Developments in Applied Phycology 6, 485-505.
770 Waldmann, N., Torfstein, A., Stein, M., 2010. Northward intrusions of low- and mid-latitude
771 storms across the Saharo-Arabian belt during past interglacials. Geology 38, 567-570.
772 Withers, N., 1983. Dinoflagellate sterols. In: Scheuer, P. (Ed.), Marine Natural Products:
773 Chemical and Biological Perspectives. Academic Press, New York, pp. 87–130.
774 Wick, L., G. Lemcke, Sturm, M., 2003. Evidence of Lateglacial and Holocene climatic change
775 and human impact in eastern Anatolia: high resolution pollen, charcoal, isotopic and
776 geochemical records from the laminated sediments of Lake Van, Turkey. The Holocene
777 13(5): 665-675.
778 Zhang, Y., Yang, P., Tong, C., Liu, X., Zhang, Z., Wang, G., Meyers, P.A., 2018. Palynological
779 record of Holocene vegetation and climate changes in a high-resolution peat profile
780 from the Xianjiang Altai Mountains, northwestern China. Quaternary Science Reviews
781 201, 111-123.

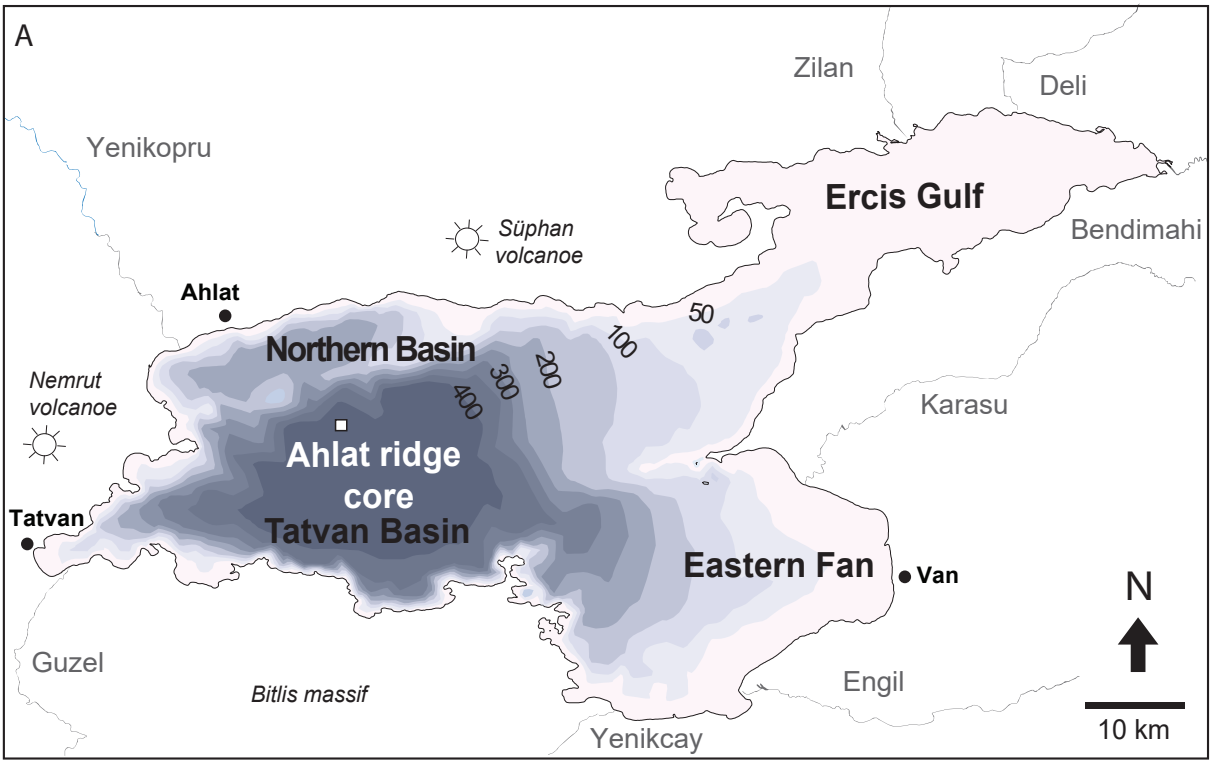
A
Zilan
Deli
Yenikopru
Ercis Gulf
Bendimahi
Süphan volcanoe
Ahlat
50
100
200
300
400
Northern Basin
Nemrut volcanoe
Karasu
Ahlat ridge core
Tatvan Basin
Tatvan
Eastern Fan
Van
N
Guzel
Bitlis massif
Engil
Yenikcay
10 km

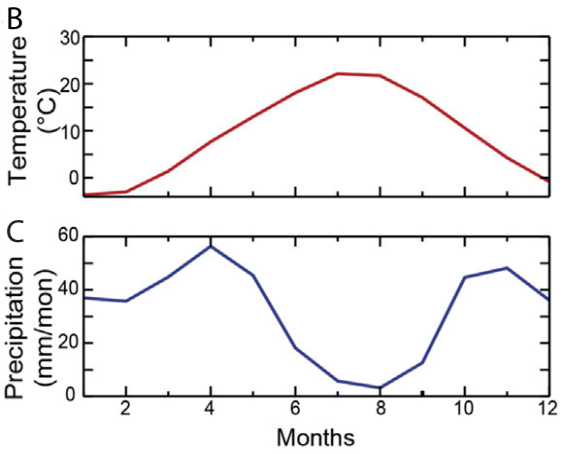
B
Temperature (°C)
30
20
10
0
C
Precipitation (mm/mon)
60
40
20
0
2
4
6
8
10
12
Months

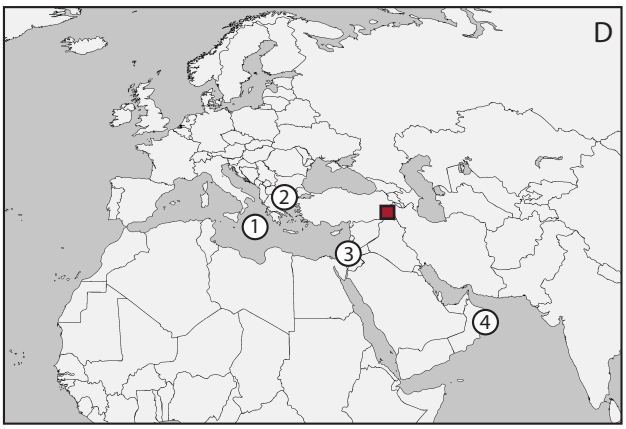
D
1
2
3
4

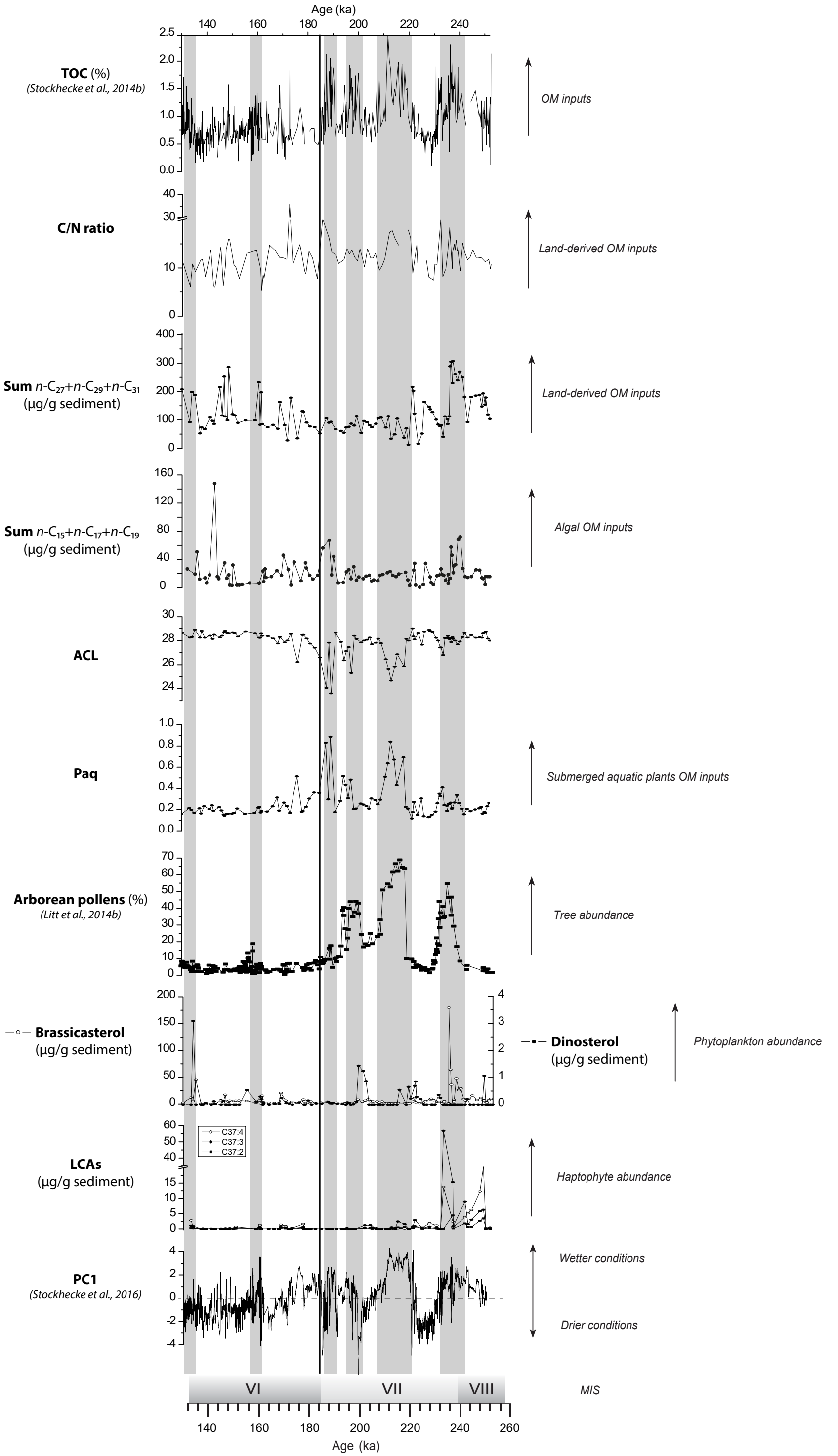
Age (ka)
140
160
180
200
220
240
TOC (%)
(Stockhecke et al., 2014b)
OM inputs
C/N ratio
Land-derived OM inputs
Sum n-C27+n-C29+n-C31
(µg/g sediment)
Land-derived OM inputs
Sum n-C15+n-C17+n-C19
(µg/g sediment)
Algal OM inputs
ACL
Paq
Submerged aquatic plants OM inputs
Arborean pollens (%)
(Litt et al., 2014b)
Tree abundance
Brassicasterol
(µg/g sediment)
Dinosterol
(µg/g sediment)
Phytoplankton abundance
LCAs
(µg/g sediment)
C37:4
C37:3
C37:2
Haptophyte abundance
PC1
(Stockhecke et al., 2016)
Wetter conditions
Drier conditions
VI
VII
VIII
MIS
Age (ka)

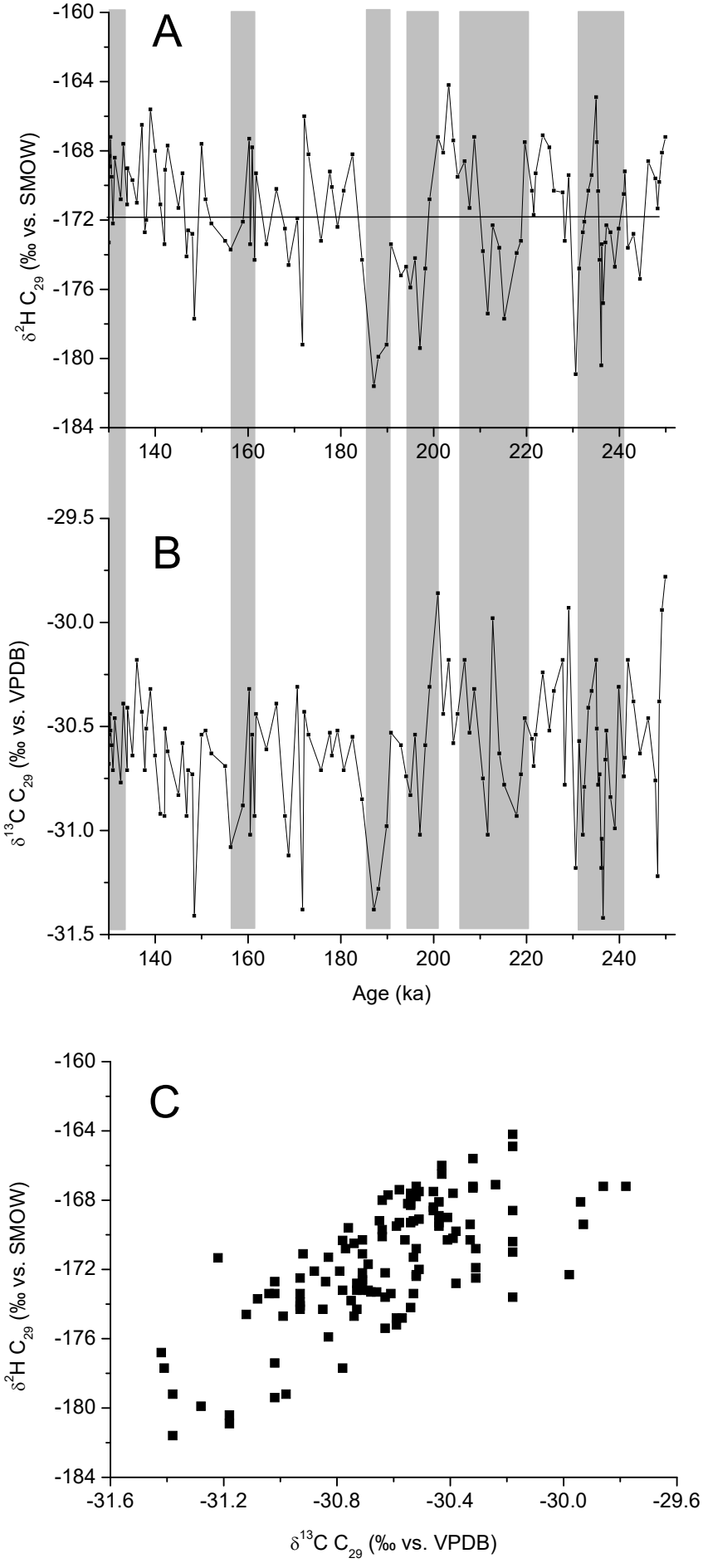
A
B
C
-160
-164
-168
-172
-176
-180
-184
140
160
180
200
220
240
-29.5
-30.0
-30.5
-31.0
-31.5
Age (ka)
δ2H C29 (‰ vs. SMOW)
δ13C C29 (‰ vs. VPDB)
-31.6
-31.2
-30.8
-30.4
-30.0
-29.6

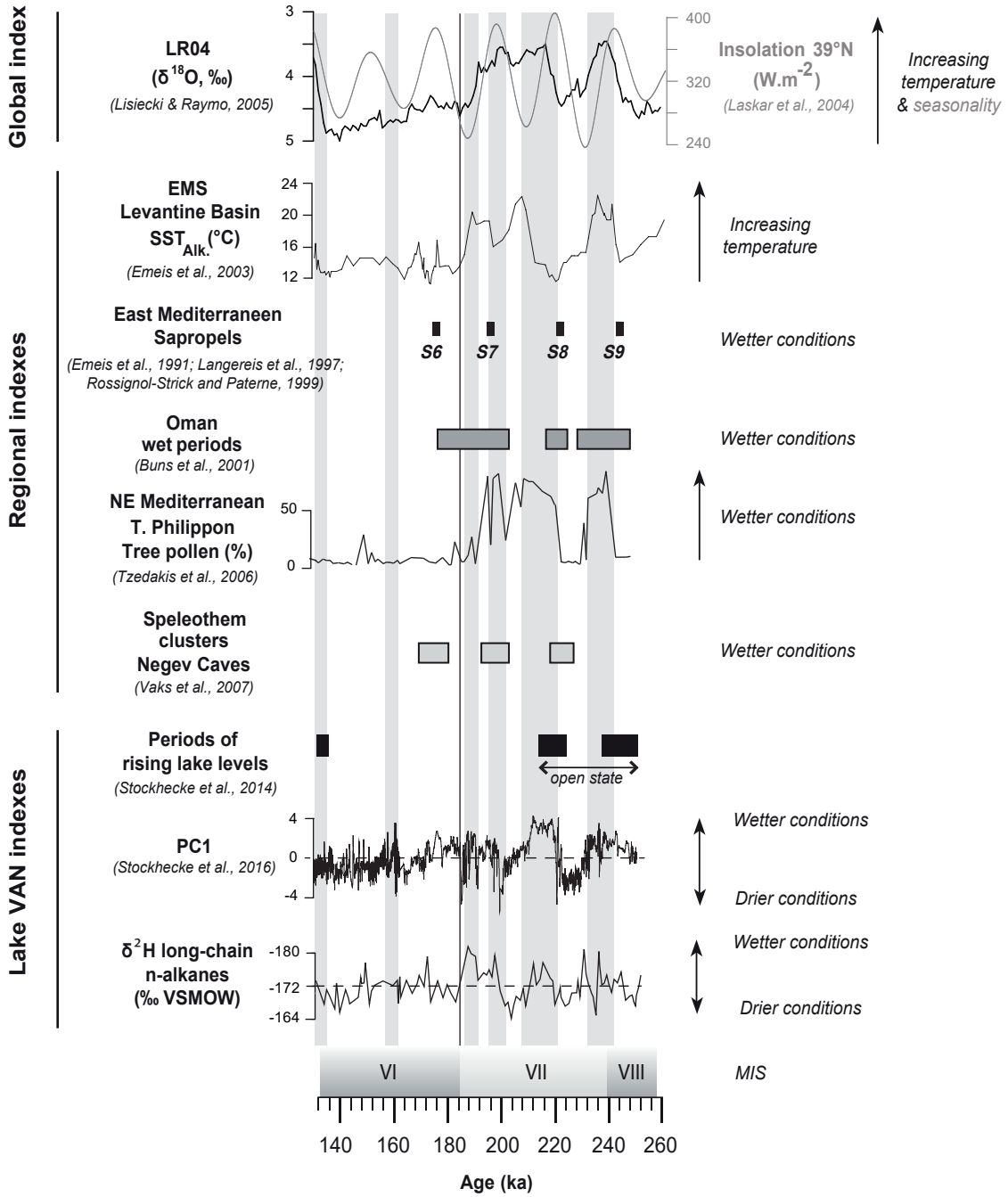
Global index
LR04
(δ18O, ‰)
(Lisiecki & Raymo, 2005)
3
4
5
400
320
240
Insolation 39°N
(W.m-2)
(Laskar et al., 2004)
Increasing
temperature
& seasonality
Regional indexes
EMS
Levantine Basin
SSTAlk.(°C)
(Emeis et al., 2003)
24
20
16
12
Increasing
temperature
East Mediterraneen
Sapropels
(Emeis et al., 1991; Langereis et al., 1997;
Rossignol-Strick and Paterne, 1999)
S6
S7
S8
S9
Wetter conditions
Oman
wet periods
(Buns et al., 2001)
Wetter conditions
NE Mediterranean
T. Philippon
Tree pollen (%)
(Tzedakis et al., 2006)
50
0
Wetter conditions
Speleothem
clusters
Negev Caves
(Vaks et al., 2007)
Wetter conditions
Lake VAN indexes
Periods of
rising lake levels
(Stockhecke et al., 2014)
open state
PC1
(Stockhecke et al., 2016)
4
0
-4
Wetter conditions
Drier conditions
δ2H long-chain
n-alkanes
(‰ VSMOW)
-180
-172
-164
Wetter conditions
Drier conditions
VI
VII
VIII
MIS
140
160
180
200
220
240
260
Age (ka)